Updating Bridge Resilience Assessment Based on Corrosion and Foundation Scour Inspection Data

Yijian Zhang[1], Reginald DesRoches[2], Iris Tien[1]

[1]School of Civil and Environmental Engineering, Georgia Institute of Technology - USA, Email: zyj.albert@gatech.edu, [2]Department of Civil and Environmental Engineering, Rice University – USA

Abstract

Aging and degradation of bridge structural components due to corrosion and scour create severe safety issues in the structural system and can lead to possible bridge failures. Collecting and analyzing inspection data provide a way to monitor and assess the safety condition of bridges. This paper proposes a framework to utilize collected inspection data to assess the condition of a bridge through updating both component- and system-level fragility curves of the bridge. Particularly, collected data such as mass loss of reinforcement and depth of scour hole are utilized to update the mechanical properties of structural members in the finite element model. Fragility curves are then updated through performing a series of nonlinear time analyses based on the inspection data. As bridges age, they are susceptible to increasing corrosion and scour. This study investigates the performance of bridges considering the combined effect of reinforcement corrosion and foundation scour under extreme loadings such as seismic events to assess bridge resilience. Fragility results quantify increases in the probabilities of damage and collapse of the structural system as measured mass loss and scour depth increase.

1. Introduction

During the life cycle of reinforced concrete (RC) highway bridges, multiple forms of aging and deterioration mechanisms may take place and impact the functionality of the bridge system. These mechanisms include the result of environmental stressors such as corrosion attack and water-induced erosion of the soil near the foundation system of bridge piles resulting in scour. Several previous studies focus on assessing the individual effects of these processes on the seismic performance of the bridges. For example, Choe et al. (2009) investigate the reduction of capacity of RC bridge columns due to corrosion and Ghosh and Padgett (2012) evaluate the impact of corrosion on bridge fragility considering multiple component deterioration and exposure conditions. Wang et al. (2014) investigate the impact of local scour on seismic fragility of bridges considering various foundation system types. Corrosion and scour are prevalent across bridges, and can act simultaneously to affect the performance of bridges, particularly in marine environments. However, there is relatively limited previous research studying the combined effect of corrosion and bridge scour on bridge fragility.

This paper presents a framework that utilizes bridge inspection data to assess bridge safety through constructing bridge fragility curves. In particular, bridge inspection data includes mass loss of reinforcement in the bridge column due to corrosion attack as well as bridge scour depth due to sustained erosion and after flooding events.

2. Mechanism and Modeling of Deterioration

2.1 Corrosion Effect

The effect of corrosion on the RC column is mainly manifested through degrading the mechanical properties of the reinforcement as well as cracking of the concrete cover due to expansion of corrosion products. Particularly, corrosion attack on reinforcement can be captured by modifying the geometric and constitutive behaviour of longitudinal reinforcement (Kashani, et al., 2015). Cracking of the concrete cover can be modeled by modifying the constitutive behaviour of unconfined concrete according to modified compression field theory (Vecchio and Collins, 1986). Details of the modeling of the effect of corrosion on bridge performance can be found in Zhang et al. (2019).

2.2 Scour Effect

Due to the erosive action of flowing water, material is carried away from the bed and banks of a stream, leading to scour. The total depth of scour consists of three components: long-term aggradation or degradation, contraction scour, and local scour. For bridges located in stream beds, due to the obstruction of the water flow by the bridge foundation system, local flow velocity and turbulence levels increase, giving rise to vortices that can remove sediment and create a scour hole around foundation system of the structure (May, et al., 2002). This paper focuses on the effect of local scour on bridges as it has been reported to significantly increase the seismic fragility of bridges (Wang et al., 2014).

The modeling of the soil-structure interaction (SSI) in this study uses the dynamic p-y method. Details regarding this method can be found in Boulanger, et al. (1999). The foundation pile is modeled as a beam on a nonlinear Winkler foundation where lateral SSI is captured by a p-y spring, and vertical axial friction and tip bearing capacity is captured by a t-z spring and q-z spring, respectively. This study considers a bridge located in sand and follows the recommendation provided by the American Petroleum Institute to calculate ultimate bearing capacity for sand. The p-y relationship is shown in Eqn. 1 below.

$$P = AP_u \tanh\left[\frac{kH}{AP_u}y\right] \qquad (1)$$

P is lateral soil resistance at any depth H, A is a modification factor that accounts for static or cyclic loading (0.9 in this case), P_u is ultimate bearing capacity at depth H, y is lateral deflection, and k is initial modulus of sub-grade reaction. The dynamic p-y method can account for the dynamic effect of SSI while maintaining reasonable computational times for probabilistic analyses (Wang et al., 2014). In this study, local scour is modeled by including both removal of the nonlinear spring along the pile as well as modifying the properties of the remaining soil due to the effects of stress history (Lin et al., 2010) and scour hole dimension (Lin et al., 2014).

3. Bridge Description and Site Conditions

The bridge selected for this study is a single-bent concrete box-girder bridge with integral pier, one of the most common bridge types in California (Mackie and Stojadinovic, 2003). A Type I pile shaft foundation is used in this bridge type, and the length of the embedded pile shaft is assumed to be 1.75 times the length of the column above grade (Wang et al., 2014). Figure 1 shows the layout of the single-frame box-girder concrete bridge. To obtain results comparable with those from previous studies, dimensions are chosen consistent with those from previous work. Table 1 summarizes the main dimensions of the two bridges considered for this selected bridge type. Further details of this bridge can be found in Mackie and Stojadinovic (2003). Uniformly graded fine sand found at the Mustang Island site is used for this study. Properties of the sand are provided in Table 2.
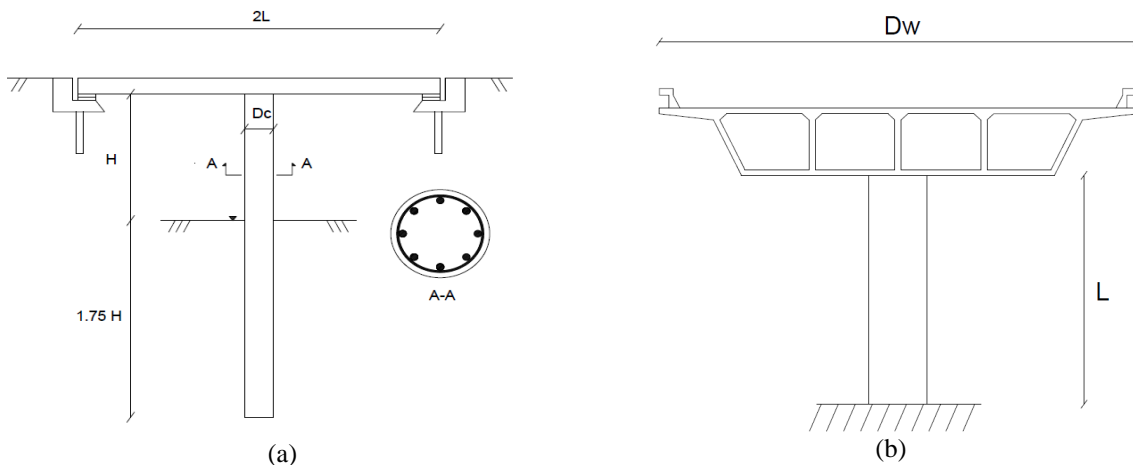

Fig. 1. (a) Longitudinal view and (b) transverse view of single-frame box-girder concrete bridge

Table 1 Dimensions of single-bent box-girder bridge

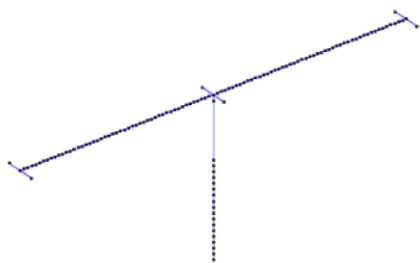| Single-bent box-girder bridge	Span Length (L), ft.	Column Height (H), ft.	Column diameter (Dc), in.
Short-span	60.0	24.6	63.0
Medium-span	120.0	32.8	79.0

Table 2 Soil Properties

Critical friction angle (°)	Effective unit weight (lb/ft³)	Relative density, (%)	Maximum void ratio	Minimum void ratio	Specific gravity
28.5	66.2	70 (Depth ≤ 3m) 90 (Depth ≥ 3m)	1.0	0.598	2.65

4. Fragility Assessment

In this section, bridge fragility considering the combined effect of corrosion and scour is assessed. First, the numerical model is built in the finite-element software OpenSees (McKenna

et al., 1997). For the sub-structure, the column is modeled using a single force-based element, and the pile foundation using multiple distribution plasticity elements with a fiber section consisting of a uniaxial constitutive model for concrete and steel. The super-structure is modeled using elastic beam-column elements. Figure 2 shows the 3D-view of the OpenSees bridge model, while Table 3 shows the dynamic properties of the short-span and medium-span bridge.

**Table 3** Dynamic properties of bridges

Unit: sec.	1st period	2nd period	3rd period
Short-span bridge	0.700	0.459	0.347
Medium-span bridge	0.916	0.527	0.499

Fig. 2. 3D-view of bridge in OpenSees

Next, analytical fragility curves are computed through running a series of nonlinear time history analyses on deterministic bridges. Similar analyses can be conducted sampling from probabilistic bridge properties. Ground motions are selected from the assembled set in Baker et al. (2011). The level of corrosion is indicated by the percentage of measured mass loss of reinforcement. The amount of scour is indicated by the measured scour depth around the bridge pier. The engineering demand parameter selected to quantify the structural damage of the bridge column is the maximum curvature. The column fragility is expressed as the probability of exceeding some damage state for a specific intensity measure. This can be expressed as a function of parameters of the capacity and demand variables assuming both of them following a lognormal distribution as shown in Eqn. (2).

$$P_f = \Phi\left(\frac{\ln S_d/S_c}{\sqrt{\xi_d^2 + \xi_c^2}}\right) \tag{2}$$

$\Phi(\cdot)$ is the standard normal cumulative distribution function. S_d and S_c are the median parameters for the demand and capacity distributions, respectively, and ξ_d and ξ_c are the lognormal standard deviation of the demand and capacity distributions, respectively. This paper presents results for the most severe damage state, collapse, defined as 20% reduction of column capacity. Figure 3 shows the resulting column fragility curves for the collapse damage state. Fragilities are calculated as a function of peak ground acceleration (PGA). Comparing across the cases considered, Figure 3 shows that the failure probability is higher for the short-span bridge at low corrosion levels, and becomes similar to that of the medium-span bridge at higher corrosion levels particularly at lower scour depths. Considering the combined effects of corrosion and scour, the effect of corrosion is more pronounced for bridges with less scour because higher levels of seismic force are experienced at bridge columns with less scour.

(a)   (b)
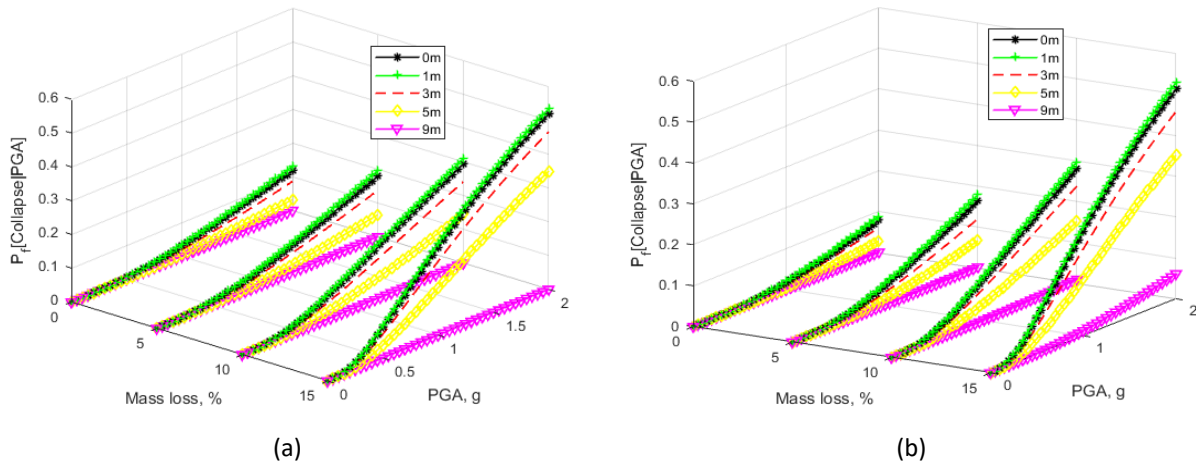
Fig. 3 Column fragility curves varying corrosion and scour levels for (a) short-span and (b) medium-span bridge

Moving from column fragility to system fragility, Figure 4 shows the bridge system fragility for the collapse damage state. System fragility curves are constructed accounting for the structural responses of individual bridge components, e.g., column curvature and deck displacement, by comparing the joint probability density functions of demand and capacity. The bridge system failure probability is computed assuming the bridge to be a series system composed of each bridge component as shown in Eqn. 3.

$$Pr[System\ Failure] = Pr[\cup_{m=1}^{M} m^{th}\ Component\ Failure] \tag{3}$$

(a)   (b)
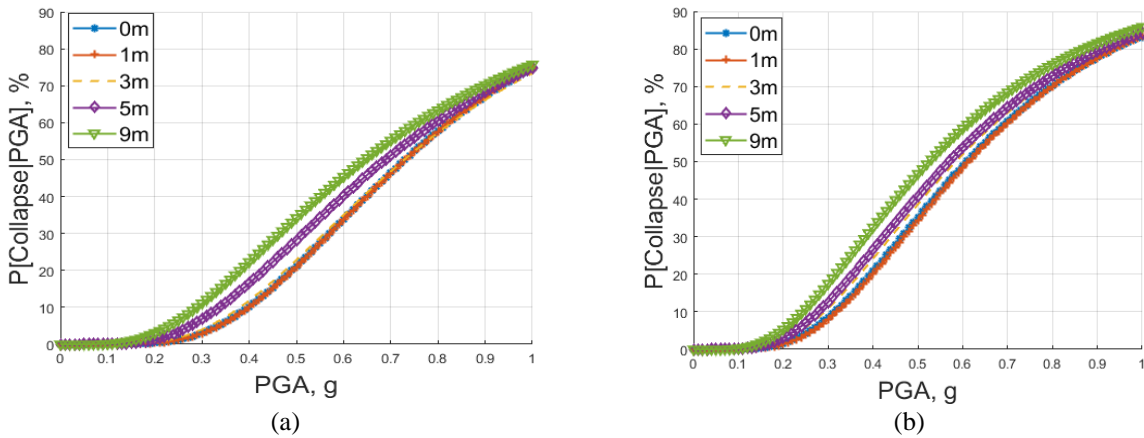
Fig. 4 System fragility curves varying corrosion and scour levels for (a) short-span and (b) medium-span bridge

For this bridge type, the system fragility curves are governed by the failure mode of unseating of the bridge deck with an increase of approximately 15% in the failure probability for 9m compared to 0m scour depth. In terms of system failure probability, the medium-span bridge is more vulnerable than the short-span bridge with higher failure probabilities given a loading intensity. This is due to the fact that the longer column contributes to larger deck displacement from rigid body rotation at the foundation.

5. Conclusions

The paper presents a framework to assess the safety condition of bridges based on collected inspection data on corrosion and scour, including measurements of mass loss of reinforcement and scour depth. Safety is evaluated as a probability of exceeding an undesired damage state under a future loading. The framework accounts for the degrading mechanical effects on reinforcement and concrete cover from corrosion and the loss of soil and effects of soil stress history and scour hole dimension under scour. To implement this framework, single-bent box-girder bridges with two geometric configurations are selected.

The results show that 15% mass loss due to corrosion increases failure probability of the bridge column by as much as 40% for both geometries. The medium-span bridge is more vulnerable at a system level at different scour hole depths due to the more slender column, with an increase in system failure probability of 15% for both geometries for a 9m compared to 0m scour hole. The effects of corrosion are more pronounced for bridges with less scour. The analysis framework presented in this paper enables updating of bridge fragility assessment under varying levels of measured corrosion and scour. In assessing the safety of bridges across a transportation network, such assessments enable identification of the most vulnerable bridges and prioritization of resources for repair or retrofit. This will decrease the vulnerability of bridges across the network and increase resilience under future loading scenarios.

6. References

Baker, J. W., Lin, T., Shahi, S. K., & Jayaram, N. (2011). New ground motion selection procedures and selected motions for the PEER transportation research program*, PEER Report*, (2011/3).

Boulanger, R. W., Curras, C. J., Kutter, B. L., Wilson, D. W., & Abghari, A. (1999). Seismic soil-pilestructure interaction experiments and analyses. *Journal of Geotechnical and Geoenvironmental Engineering*, *125*(9), 750-759.

Choe, D. E., Gardoni, P., Rosowsky, D., & Haukaas, T. (2009). Seismic fragility estimates for reinforced concrete bridges subject to corrosion. *Structural Safety*, *31*(4), 275-283.

Ghosh, J., & Padgett, J. E. (2012). Impact of multiple component deterioration and exposure conditions on seismic vulnerability of concrete bridges. *Earthquakes and Structures*, *3*(5), 649-673.

Kashani, M. M., Lowes, L. N., Crewe, A. J., & Alexander, N. A. (2015). Phenomenological hysteretic model for corroded reinforcing bars including inelastic buckling and low-cycle fatigue degradation. *Computers & Structures*, *156*, 58-71.

McKenna, F. T. (1997). Object-oriented finite element programming: frameworks for analysis, algorithms and parallel computing. (Doctoral dissertation). Berkeley, CA: University of California at Berkeley.

Lin, C., Bennett, C., Han, J., & Parsons, R. L. (2010). Scour effects on the response of laterally loaded piles considering stress history of sand. *Computers and Geotechnics*, *37*(7-8), 1008-1014.

Lin, C., Han, J., Bennett, C., & Parsons, R. L. (2014). Analysis of laterally loaded piles in sand considering scour hole dimensions. *Journal of Geotechnical and Geoenvironmental Engineering*, *140*(6), 04014024.

Mackie, K., & Stojadinović, B. (2003). *Seismic demands for performance-based design of bridges*. Berkeley: Pacific Earthquake Engineering Research Center.

May, R. W. P., Ackers, J. C., & Kirby, A. M. (2002). *Manual on scour at bridges and other hydraulic structures* (Vol. 551). London: Ciria.

Vecchio, F. J., & Collins, M. P. (1986). The modified compression-field theory for reinforced concrete elements subjected to shear. *ACI J.*, *83*(2), 219-231.

Wang, Z., Dueñas-Osorio, L., & Padgett, J. E. (2014). Influence of scour effects on the seismic response of reinforced concrete bridges. *Engineering structures*, *76*, 202-214.

Zhang, Y., DesRoches, R., & Tien, I. (2019). Impact of corrosion on risk assessment of shear-critical and short lap-spliced bridges. *Engineering Structures*, *189*, 260-271.